Formation in Solution, Synthesis, and Electrochemical Study of Oxalato Complexes of *N,N'*-Ethylenebis(salicylideneiminato)-chromium(III) and -iron(III): Crystal Structures of Piperidinium [*N,N'*-Ethylenebis(salicylideneiminato)](oxalato-O^1O^2)-chromate(III) and ferrate(III) †

Francesc Lloret, Miguel Julve, Miquel Mollar, Isabel Castro, Julio Latorre, and Juan Faus *
Departament de Química Inorgànica, Facultat de Química de la Universitat de València, Dr. Moliner 50, 46100-Burjassot (València), Spain
Xavier Solans
Departament de Cristal.lografía, Mineralogía i Dipòsits Minerals de la Universitat de Barcelona, Barcelona, Spain
Irène Morgenstern-Badarau
Laboratoire de Spectrochimie des Eléments de Transition, ERA No. 672, Université de Paris-Soud, 91405 Orsay, France

Two new mononuclear complexes of formula [Hpip][M(salen)(ox)] [M = Cr^{III} (**1**) or Fe^{III} (**2**)] and the binuclear $[Fe_2(salen)_2(ox)]\cdot H_2O$, (**3**), where Hpip = piperidinium, salen = *N,N'*-ethylenebis(salicylideneiminate), and ox = oxalate, have been synthesized. Compounds (**1**) and (**2**) are isostructural, monoclinic, space group $P2_1/n$, $Z = 4$, with $a = 24.425(3)$, $b = 6.847(1)$, $c = 14.271(2)$ Å, and $\beta = 100.95(2)°$ for (**1**) and $a = 24.363(4)$, $b = 6.991(2)$, $c = 14.105(3)$ Å, and $\beta = 98.76(2)°$ for (**2**). The structure of (**1**) was solved by direct methods whereas that of (**2**) was solved by isomorphous replacement from the co-ordinates of (**1**). Both structures consist of $[M(salen)(ox)]^-$ mononuclear anions and piperidinium cations. The presence of the bidentate oxalate ligand in both complexes forces the salen ligand to adopt the non-planar *cis*-β configuration. The metal ions exhibit distorted octahedral geometry with the two co-ordinated oxygen atoms of the oxalate ligand and an oxygen and a nitrogen atom from the salen defining the best equatorial plane. The remaining two co-ordinating atoms of the quadridentate Schiff base are bent away from the oxalate ligand. The stability constant of the complex $[Cr(salen)(ox)]^-$ as well as

$$[Cr(salen)(H_2O)_2]^+ + ox^{2-} \overset{\beta_1}{\rightleftharpoons} [Cr(salen)(ox)]^- \quad \text{(i)}$$

$$[Cr(salen)(H_2O)_2]^+ \overset{K_{a1}}{\rightleftharpoons} [Cr(salen)(OH)(H_2O)] + H^+ \quad \text{(ii)}$$

$$[Cr(salen)(OH)(H_2O)] \overset{K_{a2}}{\rightleftharpoons} [Cr(salen)(OH)_2]^- + H^+ \quad \text{(iii)}$$

the acidity constants of the complex $[Cr(salen)(H_2O)_2]^+$ have been determined by potentiometry in aqueous solution: $\log \beta_1 = 4.80 \pm 0.03$, $pK_{a1} = 7.54 \pm 0.01$, and $pK_{a2} = 10.47 \pm 0.01$ (25 °C, 0.1 mol dm^{-3} $NaNO_3$). Complexes (**1**) and (**2**) undergo one-electron reduction at a platinum electrode in dimethyl sulphoxide solution. The reduction process is totally irreversible due to an inner-sphere redox reaction in the case of Cr^{III} and to the dissociation of the anionic oxalate ligand in the case of Fe^{III}. A reactivity scheme is proposed to explain their different electrochemical behaviour.

In recent studies of iron(III) phenolate and catecholate complexes[1] as models for the catechol dioxygenases,[2] several [Fe(salen)X] complexes have been investigated where X is potentially a chelating or bridging ligand [salen = *N,N'*-ethylenebis(salicylideneiminate)]. *X*-Ray diffraction studies of such compounds have revealed the flexibility of the $Fe(salen)^+$ unit for X = acetylacetonate (acac), phenanthrene semiquinone, and catecholate (cat) anions.[3] This flexibility has been also observed in the cobalt(III) complexes [Co(salen)(acac)][4] and [Co(salen)(bzac)] (bzac = benzoylacetonate).[5] All these complexes exhibit six-co-ordination with the $salen^{2-}$ ligand adopting a *cis*-β configuration in order to accommodate the bidentate ligand. In previous papers,[6,7] we have investigated the formation of the complexes $[Fe(salen)]^+$, $[Fe(salen)(cat)]^-$, $[Fe_2(salen)_2O]$, $[Fe(saloph)(cat)]^-$, and $[Fe_2(saloph)_2O]$ [saloph = *N,N'*-(1,2-phenylene)bis(salicyclideneiminate)] in dimethyl sulphoxide (dmso)–water (80:20 w/w) solution. The high equilibrium constants for the catecholato complexes suggested the co-ordination of cat^{2-} as a bidentate ligand involving a considerable distortion of the $salen^{2-}$ and $saloph^{2-}$ ligands.

Although the complex $[Cr(salen)(H_2O)_2]^+$ was prepared 20 years ago,[8] there are only few reports on its formation of complexes in solution. Very recently, the stability constants of the complexes [Cr(Schiff base)$L(H_2O)]^+$, where L = unidentate ligand, have been determined.[9,10] Generally, few values of stability constants for chromium(III) complexes are available due to the inertness of this d^3 metal ion with regard to ligand substitution. However, kinetic studies of the interaction between $[Cr(salen)(H_2O)_2]^+$ and L have shown that the substitution of an aqua ligand in this complex occurs on the stopped-flow time-scale.[9]

† *Supplementary data available:* see Instructions for Authors, *J. Chem. Soc., Dalton Trans.*, 1989, Issue 1, pp. xvii—xx.

The structure of the complex [Hpip][Cr(salen)(ox)] (pip = piperidine, ox = oxalate) reported herein is as far as we know the first Cr^{III}–salen compound in which the salen^{2-} ligand shows the above mentioned highly distorted *cis*-β configuration.

Experimental

Reagents and Solvent.—Dimethyl sulphoxide (dmso) was purified by distillation under reduced pressure (*ca.* 2 Torr, *ca.* 266 Pa) and stored over 4-Å molecular sieves. The salt [NBu^n_4][PF_6] was recrystallized from ethanol and dried at 80 °C under vacuum. Starting materials used were [Hpip]$_2$[ox]·2H_2O,[11] [Fe(salen)(NO_3)], [Cr(salen)(H_2O)$_2$]NO_3, and [Cr(salen)(H_2O)$_2$]Cl. The complex [Fe(salen)(NO_3)], was obtained as a crystalline brown solid after refluxing for 1 h a concentrated methanol solution of Fe(NO_3)$_3$·9H_2O, H_2salen, and LiOH·H_2O in a 2:2:3 molar ratio. This simple procedure avoids the hydrolysis of [Fe(salen)]$^+$ affording [Fe(salen)(NO_3)] in a higher yield and purity than in another recently reported method[12] (Found: C, 49.95; H, 3.70; N, 10.80. Calc. for $C_{16}H_{14}FeN_3O_5$: C, 50.00; H, 3.65; N, 10.95%). The salt [Cr(salen)(H_2O)$_2$]NO_3 was obtained by a modification of the procedure described in ref. 13. A concentrated solution of Cr(NO_3)$_3$·6H_2O, H_2salen, and Na_2CO_3 (1:1:3/4 molar ratio) in ethylene glycol–water–methanol (1:1:3 w/w) was refluxed for about 5 h. On concentrating the solution a solid was obtained which was filtered off and dissolved in an aqueous sodium hydroxide solution. Yellow needle-like crystals of [Cr(salen)(H_2O)$_2$]NO_3 were obtained after neutralization of this solution by careful addition of dilute nitric acid (pH *ca.* 4) (Found: C, 46.00; H, 4.40; N, 10.20. Calc. for $C_{16}H_{18}CrN_3O_7$: C, 46.10; H, 4.30; N, 10.10%). The salt [Cr(salen)(H_2O)]Cl was prepared by a similar method to that for the preceding nitrate complex but using hydrochloric acid instead of nitric acid. This procedure avoids the reduction of Cr^{III} to Cr^{II} with zinc amalgam which was used in the previously reported method[14] (Found: C, 49.20; H, 4.70; N, 7.10. Calc. for $C_{16}H_{18}ClCrN_2O_4$: C, 49.25; H, 4.60; N, 7.20%).

Synthesis of Complexes [Hpip][M(salen)(ox)] [M = Cr^{III} (**1**) *or* Fe^{III} (**2**)].—The salt [Hpip]$_2$[ox]·2H_2O (1.2 mmol) was added to a warm methanolic solution of [Cr(salen)(H_2O)$_2$]NO_3 {or [Fe(salen)(NO_3)]} (1 mmol) and the resulting solution was refluxed for 30 min. Reddish brown crystals of complexes (**1**) and (**2**) were obtained in a high yield by slow evaporation of the corresponding solutions at room temperature. Complex (**2**) does not undergo any photochemical decomposition either as a solid or in solution in contrast to other iron(III) oxalato complexes such as K_3[Fe(ox)$_3$]·3H_2O [Found: C, 56.00; H, 5.10; N, 8.60. $C_{23}H_{26}CrN_3O_6$ (**1**) requires C, 56.10; H, 5.30; N, 8.55%. Found: C, 55.45; H, 5.25; N, 8.45. $C_{23}H_{26}FeN_3O_6$ (**2**) requires C, 55.65; H, 5.30; N, 8.45%].

Synthesis of [Fe_2(salen)$_2$(ox)]·H_2O (**3**).—This compound was obtained as a brown crystalline powder by refluxing methanolic solutions of [Fe(salen)(NO_3)] and [Hpip]$_2$[ox]·2H_2O in a 2:1 molar ratio. The product was filtered off, washed with ethanol, and stored under calcium chloride [Found: C, 54.60; H, 4.05; N, 7.50. $C_{34}H_{30}Fe_2N_4O_9$ (**3**) requires C, 54.45; H, 4.00; N, 7.45%].

Physical Techniques.—Infrared spectra were recorded on a Philips Scientific SP200 spectrophotometer as KBr pellets, and electronic spectra on a Perkin-Elmer Lambda 9 spectrophotometer in the solid state and on a Philips Scientific SP 100-8 spectrophotometer in solution. Magnetic susceptibility measurements were carried out in the range 80—300 K by using a pendulum-type apparatus[15] equipped with a nitrogen cryostat. The values reported were corrected for diamagnetic contribution estimated from Pascal's tables to be -300×10^{-6} and -299×10^{-6} e.m. units mol^{-1} for complexes (**1**) and (**2**) respectively (1 e.m. unit = S.I. $\times 10^6/4\pi$).

Potentiometric titrations were performed in a reaction vessel (capacity 70 cm^3) water-thermostatted at 25.0 ± 0.1 °C and with a nitrogen flow passing over the surface of the solution. All the measurements were carried out in 0.1 mol dm^{-3} $NaNO_3$. The titrant was delivered by a Crison 738 burette. The potentiometric measurements were made using a Radiometer PHM 84 pH-mV meter and a GK 2401C combined glass electrode. The titration system was controlled by an Apple IIe microcomputer equipped with a 9-in video display and one minifloppy disk driver. A BASIC program[16] was used to monitor, for each titration point, the e.m.f. values and the volume of titrant added. The program SUPERQUAD[17] was used to process the data and calculate both acidity and stability constants.

The electrochemical experiments were carried out in a three-electrode cell under an inert atmosphere. The working and auxiliary electrodes were platinum, the reference electrode was a saturated calomel electrode, electrically connected to the non-aqueous solution by a salt bridge containing the non-aqueous solvent (dmso) and the supporting electrolyte ([NBu^n_4][PF_6]). Cyclic voltammograms were obtained with a 305 H.Q. Instruments programming function generator which was connected to a 552 Amel potentiostat, and recorded with a Riken-Denshi F35 x-y recorder. Controlled-potential electrolysis was performed in a three-compartment cell separated by glass frits. Working and auxiliary electrodes were of platinum mesh. The charge transferred was calculated by recording intensity *versus* time and carrying out a further integration. The system was calibrated against cobaltocene, [Co(η-C_5H_5)$_2$].

Crystallography.—Diffraction data for complexes (**1**) and (**2**) were collected at 288 K with a Philips PW-1100 four-circle diffractometer using graphite-monochromated Mo-K_α radiation (λ = 0.710 69 Å). The unit-cell parameters were derived from least-squares refinement of 25 well centred reflections ($4 \leqslant \theta \leqslant 12°$). Data collection showed systematic absences ($h0l$, $h + l = 2n + 1$; $0k0$, $k = 2n + 1$) which uniquely define the monoclinic space group $P2_1/n$ for both complexes. No significant intensity decay was observed for three standard reflections measured every 2 h as orientation and intensity control. Lorentz polarization, but not absorption, corrections were made. Independent reflections with $I \geqslant 2.5\sigma(I)$ were used for the structure refinement of (**1**) and (**2**).

Structure solution and refinement. The structure of complex (**1**) was solved by direct methods using the MULTAN 84 system of computer programs,[18] whereas that of (**2**) was solved by isomorphous replacement from the co-ordinates of (**1**). Both structures were refined by full-matrix least squares with the SHELX 76 system.[19] The function minimized was $\Sigma w||F_o| - |F_c||$, where $w = \sigma(F_o) + K|F_c|$ and $K = 0.0011$ and 0.0063 for complexes (**1**) and (**2**) respectively. Twenty-two hydrogen atoms of (**1**) were located from a difference synthesis and refined with an overall isotropic thermal parameter, the remaining atoms anisotropically. Scattering factors and anomalous dispersion corrections for neutral atoms were taken from ref. 20. The refinements converged with values for R and R' listed in Table 1. The largest peaks in final Fourier difference maps were less than 0.4 and 0.5 e Å^{-3} for (**1**) and (**2**) respectively. Final atomic co-ordinates for all non-hydrogen atoms of (**1**) and (**2**) are given in Tables 2 and 3 respectively.

Additional material available from the Cambridge Crystallographic Centre comprises H-atom co-ordinates, thermal parameters, and remaining bond lengths and angles.

Table 1. Crystal data for [Hpip][M(salen)(ox)] *

Compound	M = Cr^{III} (1)	M = Fe^{III} (2)
Formula	$C_{23}H_{26}CrN_3O_6$	$C_{23}H_{26}FeN_3O_6$
M	492.5	496.3
a/Å	24.425(3)	24.363(4)
b/Å	6.847(1)	6.991(2)
c/Å	14.271(2)	14.105(3)
β/°	100.95(2)	98.76(2)
U/Å^3	2 343(1)	2 374(1)
D_c/g cm^3	1.40	1.39
F(000)	1 028	1 036
Crystal size/mm	0.10 × 0.10 × 0.15	0.80 × 0.08 × 0.10
μ(Mo-K_α)/cm^{-1}	11.65	6.98
Scan width	0.8	1.2
Reflections collected	2 296	2 186
Independent reflections [$I \geqslant 2.5\sigma(I)$]	2 153	2 052
No. of parameters refined	365	298
$R(= \Sigma\|\|F_o\| - \|F_c\|\|/\Sigma\|F_o\|)$	0.047	0.055
$R'[= (\Sigma w\|\|F_o\| - \|F_c\|\|^2/\Sigma w\|F_o\|^2)^{\frac{1}{2}}]$	0.050	0.056

* Details common to both compounds: space group $P2_1/n$; $Z = 4$; scan type, ω; scan speed 0.03° s^{-1}; θ range 2—25°.

Table 2. Final atomic co-ordinates (× 10^4; except for Cr, × 10^5) with estimated standard deviations (e.s.d.s) in parentheses for [Hpip][Cr(salen)(ox)] (1)

Atom	X/a	Y/b	Z/c
Cr	86 776(3)	8 953(12)	49 265(6)
O(1)	8 294(2)	−215(5)	5 943(3)
C(1)	7 838(3)	657(9)	6 001(4)
O(2)	7 543(2)	301(7)	6 598(3)
C(3)	7 669(3)	2 286(8)	5 259(4)
O(4)	7 242(2)	3 271(7)	5 286(3)
O(5)	7 992(1)	2 520(5)	4 672(2)
N(6)	9 278(2)	−1 171(6)	5 293(4)
C(6)	9 163(3)	−3 009(9)	4 752(5)
C(7)	8 538(3)	−3 202(9)	4 427(5)
N(7)	8 383(2)	−1 251(6)	4 008(4)
C(61)	9 688(3)	−1 057(9)	5 998(5)
C(62)	9 824(2)	571(9)	6 627(4)
C(63)	9 516(2)	2 372(8)	6 522(4)
O(63)	9 087(2)	2 694(5)	5 850(3)
C(64)	9 693(3)	3 831(9)	7 204(5)
C(65)	10 140(3)	3 615(12)	7 929(5)
C(66)	10 442(3)	1 899(14)	8 022(5)
C(67)	10 281(3)	425(12)	7 393(5)
C(71)	8 213(2)	−1 082(9)	3 101(5)
C(72)	8 232(2)	738(9)	2 608(4)
C(73)	8 605(2)	2 256(8)	3 010(4)
O(73)	8 915(1)	2 169(5)	3 871(3)
C(74)	8 670(2)	3 888(9)	2 433(4)
C(75)	8 369(3)	3 969(11)	1 504(5)
C(76)	8 010(3)	2 481(13)	1 116(5)
C(77)	7 952(2)	897(11)	1 661(5)
N(8)	6 747(2)	3 797(9)	6 816(4)
C(9)	8 541(4)	690(16)	8 487(6)
C(10)	8 994(5)	255(21)	9 371(7)
C(11)	10 620(4)	1 382(33)	10 725(9)
C(12)	10 968(5)	3 175(23)	11 061(8)
C(13)	8 612(3)	7 100(13)	8 013(6)

Table 3. Final atomic co-ordinates (× 10^4; except for Fe, × 10^5) with e.s.d.s in parentheses for [Hpip][Fe(salen)(ox)] (2)

Atom	X/a	Y/b	Z/c
Fe	87 413(3)	12 428(9)	47 901(6)
O(1)	8 357(2)	70(5)	4 903(3)
C(1)	7 918(3)	948(7)	6 072(4)
O(2)	7 622(2)	489(6)	6 636(5)
C(3)	7 742(3)	2 684(7)	5 356(4)
O(4)	7 331(2)	3 618(7)	5 468(4)
O(5)	8 071(2)	2 956(5)	4 749(4)
N(6)	9 276(2)	−1 235(6)	5 124(4)
C(6)	9 122(2)	−2 971(7)	4 549(4)
C(7)	8 455(2)	−2 852(7)	4 217(6)
N(7)	8 401(2)	−867(5)	3 795(3)
C(61)	9 644(2)	−1 448(7)	5 808(4)
C(62)	9 826(2)	67(8)	6 550(8)
C(63)	9 613(2)	2 049(7)	6 377(4)
O(63)	9 265(2)	2 590(4)	5 636(3)
C(64)	9 822(3)	3 295(8)	7 231(4)
C(65)	10 188(3)	2 857(12)	8 032(7)
C(66)	10 397(3)	890(15)	8 107(9)
C(67)	10 206(3)	−416(13)	7 334(7)
C(71)	8 196(2)	−658(6)	2 975(5)
C(72)	8 219(2)	1 163(7)	2 368(5)
C(73)	8 583(2)	2 686(7)	2 831(6)
O(73)	8 887(1)	2 576(4)	3 628(4)
C(74)	8 636(3)	4 242(7)	2 216(5)
C(75)	8 340(3)	4 360(9)	1 303(5)
C(76)	7 994(3)	2 810(11)	844(9)
C(77)	7 957(2)	1 248(9)	1 457(5)
N(8)	6 778(2)	3 194(7)	7 048(4)
C(9)	8 696(4)	−474(13)	8 404(10)
C(10)	10 941(5)	1 365(24)	10 654(11)
C(11)	10 730(5)	3 407(22)	11 065(8)
C(12)	8 802(4)	5 347(13)	8 499(8)
C(13)	8 478(3)	6 381(10)	7 663(6)

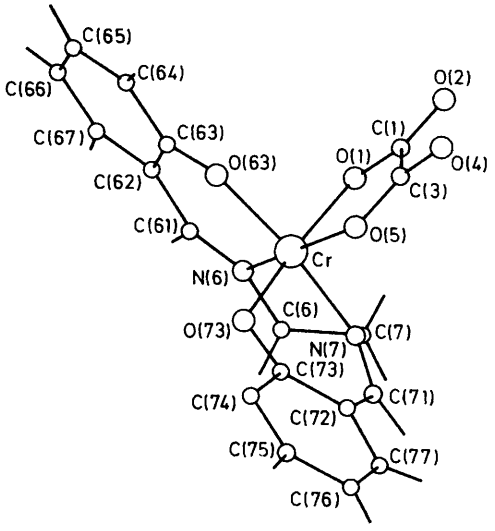

Figure 1. Perspective view of the anionic species [Cr(salen)(ox)]$^-$ with the atom numbering scheme

Results and Discussion

Molecular Structure of Complexes (**1**) *and* (**2**).—The crystals are built up mononuclear anionic species [M(salen)(ox)]$^-$ and piperidinium cations $C_5H_{12}N^+$ linked by ionic and hydrogen-bonding interactions. A perspective view of the species [Cr(salen)(ox)]$^-$ with the atomic numbering scheme is depicted in Figure 1 [the same numbering scheme has been adopted for (**2**)]. The oxalato group occupies two *cis* positions of a distorted octahedron around the metal ion, the polyhedron being completed by the quadridentate salen ligand. Selected bond distances and angles are listed in Table 4. This chelating system produces two five- and two six-membered chelate rings.

Table 4. Bond distances (Å) and angles (°) for non-hydrogen atoms of [Hpip][M(salen)(ox)]

	M = Cr^{III} (**1**)	M = Fe^{III} (**2**)		M = Cr^{III} (**1**)	M = Fe^{III} (**2**)
M–O(1)	2.019(3)	2.113(4)	C(61)–C(62)	1.431(8)	1.507(8)
M–O(5)	1.986(3)	2.020(3)	C(62)–C(63)	1.437(8)	1.487(8)
M–N(6)	2.033(5)	2.175(4)	C(63)–O(63)	1.298(6)	1.298(7)
M–N(7)	2.010(4)	2.116(5)	C(63)–C(64)	1.404(8)	1.511(8)
M–O(63)	1.937(4)	1.864(4)	C(64)–C(65)	1.362(9)	1.363(10)
M–O(73)	1.923(3)	1.965(4)	C(65)–C(66)	1.380(10)	1.465(13)
C(1)–O(1)	1.280(6)	1.285(7)	C(66)–C(67)	1.359(10)	1.444(14)
C(1)–O(2)	1.241(6)	1.195(7)	C(67)–C(62)	1.410(9)	1.372(10)
C(1)–C(3)	1.539(8)	1.596(7)	C(71)–C(72)	1.436(8)	1.540(8)
C(3)–O(4)	1.248(6)	1.225(7)	C(72)–C(73)	1.429(7)	1.473(8)
C(3)–O(5)	1.266(6)	1.272(7)	C(73)–O(73)	1.316(6)	1.250(8)
N(6)–C(6)	1.475(7)	1.476(7)	C(73)–C(74)	1.416(7)	1.410(9)
N(6)–C(61)	1.280(7)	1.222(7)	C(74)–C(75)	1.390(8)	1.378(10)
C(6)–C(7)	1.514(9)	1.624(8)	C(75)–C(76)	1.389(9)	1.462(11)
C(7)–N(7)	1.483(7)	1.508(6)	C(76)–C(77)	1.358(10)	1.404(11)
N(7)–C(71)	1.287(7)	1.197(7)	C(77)–C(72)	1.398(8)	1.347(9)
O(1)–M–O(5)	81.5(1)	78.6(1)	M–N(7)–C(7)	111.3(4)	112.2(4)
O(1)–M–O(6)	87.9(2)	81.3(2)	M–N(7)–C(71)	126.7(4)	128.3(3)
O(5)–M–N(6)	168.2(2)	159.0(2)	C(7)–N(7)–C(71)	119.7(5)	119.5(5)
O(1)–M–N(7)	92.1(2)	92.8(2)	N(6)–C(61)–C(62)	126.5(6)	124.5(5)
O(5)–M–N(7)	96.0(2)	99.3(2)	C(61)–C(62)–C(63)	123.3(5)	118.8(5)
N(6)–M–N(7)	79.1(2)	75.5(2)	C(61)–C(62)–C(67)	119.1(6)	118.6(6)
O(1)–M–O(63)	90.0(2)	93.3(2)	C(63)–C(62)–C(67)	117.6(6)	122.5(6)
O(5)–M–O(63)	94.4(1)	101.0(2)	C(62)–C(63)–O(63)	123.7(5)	125.0(5)
N(6)–M–O(63)	90.8(2)	86.3(2)	C(62)–C(63)–C(64)	116.9(5)	109.9(5)
N(7)–M–O(63)	169.5(2)	159.6(2)	O(63)–C(63)–C(64)	119.4(5)	125.0(5)
O(1)–M–O(73)	169.6(2)	164.0(2)	M–O(63)–C(63)	129.4(3)	131.9(3)
O(5)–M–O(73)	88.4(1)	86.7(2)	C(63)–C(64)–C(65)	123.1(6)	129.0(6)
N(6)–M–O(73)	101.9(2)	112.3(2)	C(64)–C(65)–C(66)	120.1(7)	116.6(9)
N(7)–M–O(73)	86.8(2)	83.1(2)	C(65)–C(66)–C(67)	119.2(7)	118.1(9)
O(63)–M–O(73)	92.9(1)	95.9(2)	C(62)–C(67)–C(66)	128.1(7)	123.6(8)
M–O(1)–C(1)	113.5(3)	115.3(3)	N(7)–C(71)–C(72)	122.4(5)	126.4(5)
O(1)–C(1)–O(2)	125.4(5)	126.7(5)	C(71)–C(72)–C(73)	120.8(5)	114.9(6)
O(1)–C(1)–C(3)	114.6(5)	113.4(5)	C(71)–C(72)–C(77)	119.1(6)	121.0(5)
O(2)–C(1)–C(3)	120.0(5)	119.6(5)	C(73)–C(72)–C(77)	119.3(6)	123.8(6)
C(1)–C(3)–O(4)	119.1(5)	118.1(5)	C(72)–C(73)–O(73)	123.5(5)	126.0(6)
C(1)–C(3)–O(5)	115.3(5)	113.8(5)	C(72)–C(73)–C(74)	118.3(5)	113.0(7)
O(4)–C(3)–O(5)	125.5(5)	128.1(5)	O(73)–C(73)–C(74)	118.1(5)	120.2(5)
M–O(5)–C(3)	114.7(4)	118.8(4)	M–O(73)–C(73)	123.1(3)	128.5(3)
M–N(6)–C(6)	113.8(4)	116.3(3)	C(73)–C(74)–C(75)	119.3(6)	122.5(6)
M–N(6)–C(61)	125.3(4)	127.6(4)	C(74)–C(75)–C(76)	122.0(7)	123.6(6)
C(6)–N(6)–C(61)	120.4(5)	115.4(4)	C(75)–C(76)–C(77)	119.0(6)	112.9(9)
N(6)–C(6)–C(7)	108.4(5)	106.0(4)	C(72)–C(77)–C(76)	122.1(6)	123.8(7)
C(6)–C(7)–N(7)	102.2(5)	100.6(4)			

The short bond angles around the metal ion in the five-membered rings [N(7)–M–N(6) and O(1)–M–O(5) 79.1(2) and 81.5(1)° for (**1**) and 75.5(2) and 78.6(1) for (**2**)] cause a deviation from the ideal 90° value in the angles N(7)–M–O(5), O(63)–M–O(5), and O(73)–M–N(6) [96.0(2), 94.4(1), and 101.9(2)° in (**1**) and 99.3(2), 101.0(2), and 112.3(2)° in (**2**)].

The best equatorial plane is defined by the O(1) and O(5) atoms of the oxalate ligand and N(6) and O(73) atoms of the $salen^{2-}$ [average deviations 0.072(4) and 0.134(4) Å for complexes (**1**) and (**2**) respectively]. The non-planar *cis*-β configuration [21] which the salen ligand exhibits in both structures is due to the accommodation of the co-ordinated bidentate ligand; this results in the rotation of a phenyl–imine nitrogen bond and the displacement of O(73) by 1.807(7) Å in (**1**) [1.652(7) Å in (**2**)] from the plane defined by the chromium atom (iron atom) and the other three co-ordinating atoms in the $salen^{2-}$. The interplanar angle between the salicylidene rings is 48.6(6) and 38.9(6)° for (**1**) and (**2**) respectively, the imine-nitrogen atom being tetrahedrally distorted. This distortion is also reflected in the metal–ligand bond lengths of (**2**) where the 'equatorial' Fe–N(6) and Fe–O(73) bonds are longer than the corresponding 'axial' ones. These structural features are also present in (**1**) but to a lower degree. A comparison of the distortions observed in several salen complexes relative to the undistorted five-co-ordinate iron complex $[Fe_2(salen)_2(hq)]$ (hq = hydroquinonate) is shown in Table 5. The interplanar angle increases from 8.4° in this compound to 58.6° for [Co(salen)(acac)], whereas the imine torsional angle decreases from 177° in the five-co-ordinate complex to 153° in the cobalt complex. The iron complexes exhibit varying degrees of distortion toward the *cis*-β configuration depending on the bidentate ligand, X.

The metal–oxygen bond distances with the oxalate ligand are longer than those with the phenolic oxygen atoms and alter according to the *trans* atoms. This is also true of the metal–nitrogen bond angles. The two iron–phenolic oxygen atom distances, Fe–O(63) and Fe–O(73), are significantly different [1.864(4) and 1.965(4) Å], as has been observed in [Fe(salen)(acac)].[3] However, these distances are nearly identical in the complexes K[Fe(salen)(cat)][3] and [Fe(salen)(psq)][3] (psq = phenanthrene semiquinone) as well as in the complex (**1**) reported herein, all of them exhibiting the non-

Table 5. Bond angles (°) for various salen complexes

Complex	Imine torsion angle	Salen–salen interplanar angle	Salen N–M–O angles 'axial'	'equatorial'	Ref.
$[Fe_2(salen)_2(hq)]$	179, 177	8.4	144	154	22
[Fe(salen)(psq)]	178, 171	28.1	159	117	3
$[Fe(salen)(cat)]^-$	179, 163	39.8	155	110	3
[Fe(salen)(acac)]	180, 183	52.6	160	106	3
[Co(salen)(acac)]	180, 153	58.6	176	97	4*b*
$[Fe(salen)(ox)]^-$	178, 173.7	38.9	159.6	112.3	This work
$[Cr(salen)(ox)]^-$	177.8, 169	48.6	169.5	101.9	This work

Table 6. Possible hydrogen-bonding interactions, A–H · · · D, for [Hpip][M(salen)(ox)]

M	A	D	Equivalent position for D	A–D/Å	A–H · · · D/°
Cr(**1**)	N(8)	O(2)	$\frac{3}{2} - x, y + \frac{1}{2}, \frac{3}{2} - z$	2.815(7)	161.0(5)
	N(8)	O(4)	x, y, z	2.653(7)	164.0(5)
Fe(**2**)	N(8)	O(2)	$\frac{3}{2} - x, y + \frac{1}{2}, \frac{3}{2} - z$	2.708(7)	
	N(8)	O(4)	x, y, z	2.791(7)	

planar *cis*-β configuration. The values of the metal–imine nitrogen bond distances reveal that Cr^{III} has a greater affinity for the imine groups than Fe^{III} [averages, 2.02 and 2.15 Å for (**1**) and (**2**) respectively]. The same trend is observed when comparing the structures of the complexes $[Cr(salen)(H_2O)_2]Cl$[14] and $[Fe_2(salen)_2Cl_2]$.[23] The values of the M–O(1) and M–O(5) bond lengths lead to the same conclusion regarding the oxalate ligand. The oxalate shows double-bond character in C(1)–O(2) and C(3)–O(4), O(2) and O(4) being the unco-ordinated oxygen atoms. A more important double-bond character is observed in (**2**) which promotes a lengthening of the C(1)–C(3) bond distance [1.596(7) Å in (**2**) *versus* 1.539(8) Å in (**1**), whereas the C(1)–O(1) and C(3)–O(5) distances are very similar in the two structures].

By comparison to $K_3[Fe(ox)_3]\cdot 3H_2O$[24] and $K_3[Cr(ox)_3]\cdot 3H_2O$,[25] the metal–oxalate interaction in complexes (**1**) and (**2**) is somewhat weaker {average values for M–O(oxalate) bond are 2.00 and 1.90 Å for $[Cr(salen)(ox)]^-$ and $[Cr(ox)_3]^{3-}$ and 2.07 and 2.04 Å for $[Fe(salen)(ox)]^-$ and $[Fe(ox)_3]^{3-}$ respectively}.

Hydrogen-bonding interactions in complexes (**1**) and (**2**) are given in Table 6: the unco-ordinated oxygen atoms of the oxalate ligand are hydrogen bonded to two piperidinium cations.

I.r. and Electronic Spectra.—The i.r. bands attributable to the oxalate ligand in the region 1 750—1 250 cm^{-1} for some mononuclear oxalato-chromium(III) and -iron(III) complexes and two binuclear oxalato-bridged iron(III) complexes are given in Table 7. The splitting of the $\nu_{asym}(CO)$ and $\nu_{sym}(CO)$ stretching vibrations observed for the mononuclear complexes is characteristic of the bidentate oxalate ligand.[26] However, no splitting is observed for the carbon–oxygen stretching vibrations of the binuclear species. This feature strongly suggests that these stretching vibrations could serve as a diagnostic for the bidentate or bis(bidentate) co-ordination mode of the oxalate ligand.

A good agreement is observed between the methanolic solution and diffuse reflectance spectra of complex (**1**) suggesting that the environment of chromium(III) is substantially the same in the two cases. Assuming that the symmetry of this complex approximates to O_h, the band at 18 500 cm^{-1} (ε = 68.9 $dm^3\ mol^{-1}\ cm^{-1}$) can be assigned to the transition $^4A_{2g} \longrightarrow {}^4T_{2g}$, so it will be approximately $10Dq$. The complex

Table 7. I.r. bands (cm^{-1}) attributable to the oxalate ligand in the region 1 750—1 250 cm^{-1}

Complex	$\nu_{asym}(CO)$	$\nu_{sym}(CO)$	Ref.
(**1**) [Hpip][Cr(salen)(ox)]	1 725 (sh), 1 670, 1 640vs	1 445, 1 295s	This work
(**2**) [Hpip][Fe(salen)(ox)]	1 730 (sh), 1 685, 1 650vs	1 445, 1 300s	This work
$K_3[Cr(ox)_3]\cdot 3H_2O$	1 708 (sh), 1 684, 1 660vs	1 387, 1 253s	26
$K_3[Fe(ox)_3]\cdot 3H_2O$	1 712(sh), 1 677, 1 649vs	1 390, 1 270, 1 255s	26
(**3**) $[Fe_2(salen)_2(ox)]\cdot H_2O$	1 665vs	1 340m	This work
$[Fe_2(acac)_4(ox)]\cdot 0.5H_2O$	1 650vs	1 320m	11

Table 8. Ligand field splitting for several octahedral chromium(III) complexes

Compound	$10Dq/cm^{-1}$	Ref.
$[Cr(en)_2(ox)]^+$	20 200	27
cis-$[Cr(en)_2(H_2O)_2]^{3+}$	20 600	*
$[Cr(ox)_3]^{3-}$	17 500	*
$[Cr(H_2O)_6]^{3+}$	17 400	*
$[Cr(salen)(H_2O)_2]^+$	21 500	This work
$[Cr(salen)(OH)_2]^-$	21 800	This work
$[Cr(salen)(ox)]^-$	18 500	This work

* H. L. Schlafer, *Z. Phys. Chem.* (*Frankfurt*), 1957, **11**, 65.

$[Cr(salen)(H_2O)_2]^+$ exhibits this transition at 21 500 cm^{-1} (ε = 170 $dm^3\ mol^{-1}\ cm^{-1}$), and the related complexes $[Cr(salen)(OH)(H_2O)]$ and $[Cr(salen)(OH)_2]^-$ absorb in the same region. If these values of $10Dq$ are correct then the transition to the $^4T_{1g}(P)(O_h)$ term would be expected to lie in the region of 35 000 cm^{-1} for (**1**) and 38 000 cm^{-1} for $[Cr(salen)(H_2O)_2]^+$. Some bands were observed in these regions in the solution spectra but they have high absorption coefficients and cannot reliably be assigned to this transition. When comparing values of $10Dq$ for chromium(III) oxalato complexes with ones for chromium(III) aqua complexes (Table 8) it is inferred that the ligands oxalate and aqua give rise to similar ligand-field splitting for $Cr^{III}(O_h)$. So, the smaller value of $10Dq$ of complex (**1**) with respect to that of *trans*-$[Cr(salen)(H_2O)_2]^+$ indicates that the salen ligand in a planar conformation gives rise to a stronger ligand-field splitting than when it adopts a *cis*-β configuration.

The absorption spectra of iron(III) complexes (**2**) and (**3**) are very similar. They consist of intense charge-transfer bands in the visible region and a weak band at 8 300 cm^{-1}. This last band can be attributed to the spin-forbidden transition $^6A_{1g} \longrightarrow {}^4T_{1g}$

Table 9. Room-temperature values of $\mu_{eff.}$[a] and estimated t.i.p.[b] contribution

Compound	$\mu_{eff.}$	10^{-6} t.i.p.	$\mu_{eff.}^{cor}$ [c]	Ref.
$[Cr(salen)(H_2O)_2]Cl$	3.86	250	3.78	14
$K[Cr(salen)(OH)_2]\cdot 4H_2O$	3.87	250	3.79	14
(1) [Hpip][Cr(salen)(ox)]	3.91	150	3.86	This work

[a] At 300 K. [b] In c.g.s. units. [c] $\mu_{eff.}$ − t.i.p.

taking into account the octahedral environment of Fe^{III} in (**2**). Since this transition is also present in the spectrum of (**3**), it can be concluded that the environment of Fe^{III} in this complex will be very similar to that of (**2**). It is not possible to determine $10Dq$ for (**2**) because only one *d*–*d* transition is observed ($^6A_{1g} \longrightarrow {}^4T_{1g}$) the energy of which is dependent upon $10Dq$, B, and C. However, $10Dq$ can be calculated as a semiempirical parameter from Jørgensen's relation[27] [equation (1)]. The value of

$$10Dq = f(\text{ligand}) \times g(\text{metal ion}) \qquad (1)$$

f(ligand) was calculated from the $10Dq$ value measured for complex (**1**) (Cr^{III} with the same ligands). The values of $g(Fe^{III})$ and $g(Cr^{III})$ were taken as 14.0 and 17.4 respectively.[27] So, a value of 14 900 cm^{-1} was obtained for $10Dq$ of (**2**).

Magnetic Properties.—Measurements of the molar magnetic susceptibility, χ_M, of complex (**1**) over the temperature range 300—80 K reveal that this complex strictly obeys the Curie law as do $[Cr(salen)(H_2O)_2]Cl$ and $K[Cr(salen)(OH)_2]\cdot 4H_2O$.[14] The values of $\mu_{eff.}$ at 300 K and the temperature-independent paramagnetism (t.i.p.) which have been obtained from the experimental values of the magnetic susceptibility are given in Table 9. Mononuclear chromium(III) complexes with O_h symmetry have a $^4A_{2g}$ ground term and its magnetic properties are modified by its interaction with the excited $^4T_{2g}$ term *via* spin–orbit coupling and the magnetic field, leading to $\mu_{eff.} = \mu_{so}[1 - 4\lambda/10Dq]$ and a t.i.p. contribution to the magnetic susceptibility of $8k^2N\beta^2/10Dq$. The value of the spin-only magnetic moment for Cr^{III} (d^3) is 3.872 B.M. Since the spin–orbit coupling constant of Cr^{III} is 90 cm^{-1} and $10Dq$ for (**1**) is about 18 500 cm^{-1}, the reduction in the magnetic moment is only *ca.* 2% and a t.i.p. value of 120 × 10^{-6} c.g.s. units can be deduced. So, the calculated values are in good agreement with the experimental ones (see Table 9).

Measurements of χ_M for complex (**2**) over the temperature range 300—80 K give a value of 5.75 for $\mu_{eff.}$ indicating a high-spin complex. However, magnetic and e.s.r. studies which some of us are carrying out on this complex over the temperature range 80—4 K reveal that the ground state could be described as a quantum mechanically mixed-spin state arising from $S = \frac{3}{2}$ and $\frac{5}{2}$ states.[28]

Deprotonation Equilibria of $[Cr(salen)(H_2O)_2]^+$.—The compounds $[Cr(salen)(H_2O)_2]Cl$ and $[Cr(salen)(H_2O)_2]NO_3$ are moderately soluble in water, but they are highly soluble in methanol yielding yellow-brown solutions. Conductivity measurements in both solvents show that chloride and nitrate ions are unco-ordinated, so $[Cr(salen)(H_2O)_2]^+$ must be the only complex existing in solution. These solutions are stable, strictly obey Beer's law, and do not undergo any decomposition on addition of strong acids. Moreover, a colour change from yellow-brown to red occurs when sodium hydroxide is added. Reaction is complete when 2 mol of OH^- per mol of $[Cr(salen)(H_2O)_2]^+$ are added and the resulting spectrum is identical to the reflectance spectrum of the solid $K[Cr(salen)(OH)_2]\cdot 4H_2O$.[14] All these data enable us to conclude that reactions (2) and (3) occur. These hydroxo-complexes are very

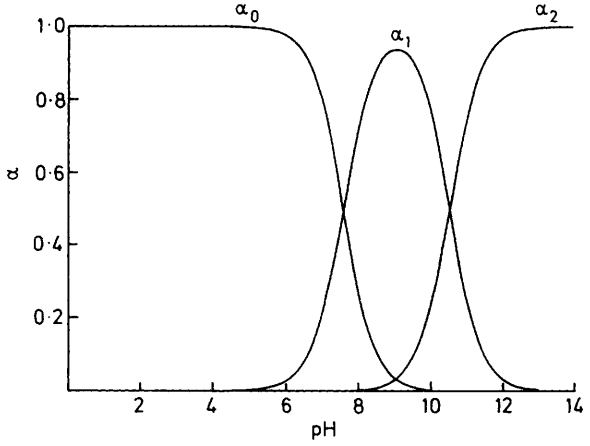

Figure 2. Distribution diagram for the species in an aqueous solution of $[Cr(salen)(H_2O)_2]^+$ as a function of pH; α is the ratio between the concentration of each species and the initial concentration of $[Cr(salen)(H_2O)_2]^+$, $\alpha_0 = [Cr(salen)(H_2O)_2]^+$, $\alpha_1 = [Cr(salen)(OH)(H_2O)]$, and $\alpha_2 = [Cr(salen)(OH)_2]^-$

$$[Cr(salen)(H_2O)_2]^+ \overset{K_{a1}}{\rightleftharpoons} [Cr(salen)(OH)(H_2O)] + H^+ \qquad (2)$$

$$[Cr(salen)(OH)(H_2O)] \overset{K_{a2}}{\rightleftharpoons} [Cr(salen)(OH)_2]^- + H^+ \qquad (3)$$

soluble in aqueous solution. In order to determine the values of the acidity constants, K_{a1} and K_{a2}, aqueous solutions of $[Cr(salen)(H_2O)_2]^+$ as a chloride or nitrate salt were titrated potentiometrically with NaOH (*ca.* 0.1 mol dm^{-3}). The initial concentration of $[Cr(salen)(H_2O)_2]^+$, c_M, was varied in the range 5 × 10^{-4}—2 × 10^{-3} mol dm^{-3}. The values of K_{a1} and K_{a2} were computed by the program SUPERQUAD.[17] In the calculations we used 90 experimental points from three different experiments. The values obtained for pK_{a1} and pK_{a2} are 7.54 ± 0.01 and 10.47 ± 0.01 respectively. The distribution diagram for the species existing in solution is depicted in Figure 2.

Prasad *et al.*[9,10] determined spectrophotometrically the value of pK_{a1} [equation (2)] as 8.04 (25 °C, 1 mol dm^{-3} $LiClO_4$). The noticeable difference between this value and the corresponding one reported herein could be attributed to the different nature and concentration of the background electrolyte used.

Although the complex $[Cr(salen)(OH)_2]^-$ had been isolated and characterized as a sodium or potassium salt,[14] its formation in solution has not been studied. The potentiometric study we have carried out has allowed us to determine its formation constant. According to this study this complex exists as the only species at pH > 12 (Figure 2). The complex $[Cr(salen)(H_2O)(OH)]$ is the only species existing in solution at pH 9. Attempts to isolate this mononuclear species led to the precipitation of a red-brown solid with stoicheiometry 'Cr(salen)(OH)' which is insoluble in most common solvents and exhibits an antiferromagnetic exchange interaction.[14] These facts strongly support a polymeric nature for this complex but the lack of an *X*-ray structure determination prevents its elucidation.

The complex $[Fe(salen)]^+$ exhibits a very different behaviour in a basic medium yielding a μ-oxo complex of formula $[Fe_2(salen)_2O]$[6b] according to reaction (4). This reaction

$$2[Fe(salen)]^+ + 2OH^- \rightleftharpoons [Fe_2(salen)_2O] + H_2O \qquad (4)$$

Table 10. Metal–nitrogen (imine) and –oxygen (phenolato) bond distances (averages in Å) for several salen complexes

Compound	M–N (imine)	M–O (phenolato)	Ref.
(1) [Hpip][Cr(salen)(ox)]	2.02	1.93	This work
(2) [Hpip][Fe(salen)(ox)]	2.15	1.92	This work
$[Cr(salen)(H_2O)_2]Cl$	2.00	1.93	14
$[Fe_2(salen)_2Cl_2]$	2.10	1.94	23
[Cu(salen)]	2.01	1.97	*

* D. Hall and T. N. Waters, *J. Chem. Soc.*, 1960, 2644.

proceeds probably by deprotonation of one axial H_2O ligand and condensation between two Fe(salen)(OH) units. However, there is no evidence of the existence in equilibrium of hydroxo-complexes in significant concentrations.[6b]

The complex $[Cr(salen)(H_2O)_2]^+$ is stable in an acidic medium, being the only species existing in aqueous solution at pH < 6. In contrast, $[Fe(salen)]^+$ is unstable in acidic media undergoing hydrolytic decomposition[6b] to salicylaldehyde (Hsal) and ethylenediammonium (H_2en^{2+}) [equation (5)]. The

$$[Fe(salen)]^+ + 4H^+ \rightleftharpoons Fe^{3+} + 2Hsal + H_2en^{2+} \quad (5)$$

different stability of the salen complexes of Cr^{III} and Fe^{III} with respect to this hydrolytic decomposition in acidic media is due probably to the known inertness to ligand substitution of the complexes of Cr^{III} (O_h). However, the possibility of a greater thermodynamic stability for $[Cr(salen)(H_2O)_2]^+$ cannot be ruled out. So, this greater stability could have its origin in the higher affinity of Cr^{III} with respect to Fe^{III} for imine-nitrogen atoms, whereas the affinity of the metal ions for the phenolate-oxygen atoms should not be very different. Structural data gathered in Table 10 support these considerations. So, for instance, the greater affinity of Cu^{II} with regard to Fe^{III} for the imine-nitrogen atoms explains the analogous stability of complexes [Cu(salen)] and $[Fe(salen)]^+$ (log β = 27.32 and 25.85 respectively) in spite of the greater affinity of Fe^{III} for the phenolate-oxygen atoms.

Formation of [M(salen)(ox)] (M = Cr^{III} *or* Fe^{III}).—We have studied spectrophotometrically the interaction between $[Cr(salen)(H_2O)_2]^+$ and oxalate in methanolic solution. A colour change from yellow to red occurs when piperidinium oxalate is added to a methanolic solution of $[Cr(salen)(H_2O)_2]^+$. The spectra display an isosbestic point at 525 nm which indicates the presence of two absorbing species in solution. The application of the molar ratio method shows the formation of only a 1:1 complex [equation (6)]. This complex

$$[Cr(salen)(H_2O)_2]^+ + ox^{2-} \rightleftharpoons [Cr(salen)(ox)]^- + 2H_2O \quad (6)$$

strictly obeys Beer's law and its absorption spectrum is identical to the reflectance one of the solid [Hpip][Cr(salen)(ox)]. The stability constant was determined by potentiometry in aqueous solutions. Solutions of $[Cr(salen)(H_2O)_2]^+$ as a chloride or nitrate salt with various concentrations ($c_M = 5 \times 10^{-4}$–2×10^{-3} mol dm^{-3}) were titrated with oxalic acid (*ca.* 10^{-2} mol dm^{-3}). Previously, we have determined the acidity constants of oxalic acid ($pK_{a1} = 1.03 \pm 0.01$ and $pK_{a2} = 3.80 \pm 0.01$). The program SUPERQUAD was used to process data and calculate the stability constant; 70 experimental points from three independent experiments were used. The value obtained is log $K = 4.80 \pm 0.03$ and the distribution diagram is shown in Figure 3. The complex is completely formed at pH > 3, being stable until pH *ca.* 8. At pH > 8 it decomposes yielding the corresponding hydroxo-complexes. At pH ≥ 11 dissociation of the complex is complete and $[Cr(salen)(OH)_2]^-$ is the only existing species.

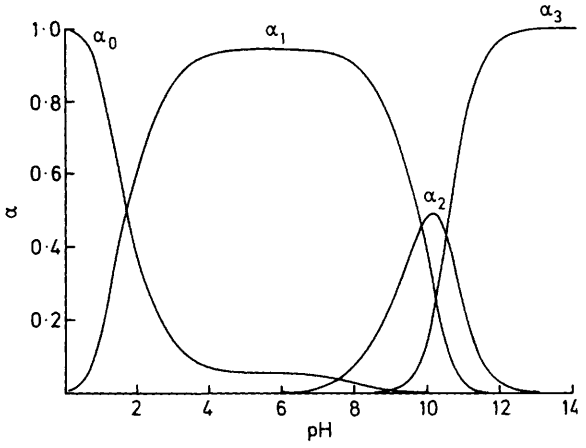

Figure 3. Distribution diagram (α *versus* pH) for the system $[Cr(salen)(H_2O)_2]^+ - ox^{2-}$: $\alpha_0 = [Cr(salen)(H_2O)_2]^+$, $\alpha_1 = [Cr(salen)(ox)]^-$, $\alpha_2 = [Cr(salen)(OH)(H_2O)]$, and $\alpha_3 = [Cr(salen)(OH)_2]^-$. Concentrations c_M and c_L are 5×10^{-3} mol dm^{-3}

In contrast with the inertness of the complex $[Cr(ox)_3]^{3-}$ to ligand substitution, $[Cr(salen)(ox)]^-$ exhibits a higher lability in MeOH or water at room temperature. Since the oxalate ligand co-ordinates and dissociates instantaneously, it seems that the planar–*cis*-β octahedral conformational change of the ligand $salen^{2-}$ does not present any significant energy barrier at room temperature. Such a high kinetic lability allowed us to study the complex formation by conventional potentiometry. However, the formation reaction takes place slowly if dmso is used as the solvent. Although the substitution inertness of Cr^{III} (d^3) ion in aqua-ligand environments is well known, the complex $[Cr(salen)(H_2O)_2]^+$, as well as [Cr(edta)$(H_2O)]^-$ (edta = ethylenediaminetetra-acetate) and [Cr(tpps)$(OH)(H_2O)]^{4-}$ [tpps = *meso*-tetra(*p*-sulphonatophenyl)-porphyrinate], exhibit substitution of co-ordinated water at stopped-flow rates due to a ground-state distortion.[9,10,29,30] The kinetic study of the reactions represented by equation (7)

$$[Cr(salen)(H_2O)_2]^+ + L^{n-} \rightleftharpoons [Cr(salen)(H_2O)L]^{1-n} + H_2O \quad (7)$$

has afforded the equilibrium constants of Cr^{III}–salen complexes with various unidentate ligands (see Table 11). However, to our knowledge no study has been carried out on the formation of the parent complexes $[Cr(salen)L_2]^{1-2n}$ nor with bidentate ligands. So, the study of the complex $[Cr(salen)(ox)]^-$ has allowed us to determine for the first time the stability constant of the complex $[Cr(salen)(H_2O)_2]^+$ with a bidentate ligand, revealing the lability of both water molecules in aqueous solution. As shown in Table 11, the stability constant of the complex $[Cr(salen)(ox)]^-$ is much greater than the ones corresponding to the interaction with unidentate ligands and of the same order as the stepwise formation constants of the complex $[Cr(ox)_3]^{3-}$.

Unfortunately, we could not carry out a study of the formation of the complex $[Fe(salen)(ox)]^-$ similar to that described for Cr^{III}, due to the decomposition of $[Fe(salen)]^+$ in acidic media. However, the absorption spectra of methanolic solutions of $[Fe(salen)]^+$–ox^{2-} with different ratios x =

Table 11. Stability constants[a] of several complexes of Cr^{III}

Equilibrium	Log K	Ref.
$[Cr(salen)(H_2O)_2] + L \rightleftharpoons [Cr(salen)(H_2O)_nL]$	1.2 (L = SCN^-, n = 1)	9, 10
	1.4 (L = N_3^-, n = 1)	9, 10
	2.0 (L = py, n = 1)[b]	9, 10
	4.80 (3) (L = ox^{2-}, n = 0)	This work
$[Cr(ox)_n] + ox \rightleftharpoons [Cr(ox)_{n+1}]$	5.34 (n = 0)	[c]
	5.17 (n = 1)	[c]
	4.93 (n = 2)	[c]

[a] Charges are omitted in the equilibria for simplicity. [b] py = Pyridine. [c] K. Nagata, A. Umayahara, and K. Tsuchiya, *Bull. Chem. Soc. Jpn.*, 1965, **38**, 1059.

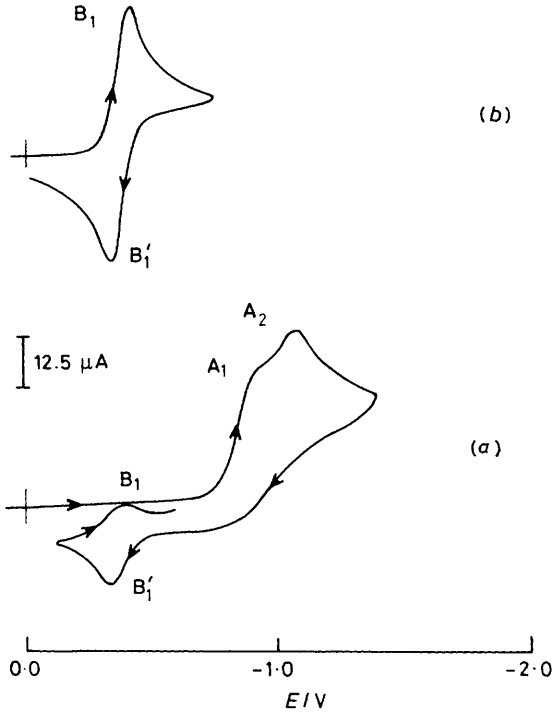

Figure 4. Cyclic voltammograms for (*a*) $[Fe(salen)(ox)]^-$ and (*b*) $[Fe(salen)]^+$. Scan rate 100 mV s^{-1} and 0.2 mol dm^{-3} $[NBu^n_4][PF_6]$

$[ox^{2-}]/[Fe(salen)^+]$ (x = 0—1) reveal the existence of more than two absorbing species. When x = 0.5 a red-brown solid is easily obtained as a crystalline powder. It is highly insoluble in MeOH and both chemical analysis and spectroscopic characterization indicate the μ-oxalato complex $[Fe_2(salen)_2(ox)]\cdot H_2O$ (**3**). This binuclear complex dissolves easily when oxalate is added to yield $[Fe(salen)(ox)]^-$ at x = 1. In basic media, dissociation of co-ordinated oxalate leads to the formation of the μ-oxo complex $[Fe_2(salen)_2O]$ which precipitates as an orange solid.

Electrochemical Study.—Cyclic voltammetry on complex (**2**) in dmso solution shows two totally irreversible reductions peaks A_1 and A_2 at −0.90 and −1.06 V respectively, Figure 4(*a*) (s.c.e. reference). However, an oxidation process B_1' is detected at −0.34 V in the reverse sweep. This process can be considered as a typical electrochemical reversible system and has been identified as the redox couple Fe^{III}(salen)–Fe^{II}(salen) by comparison with the redox behaviour of a sample of

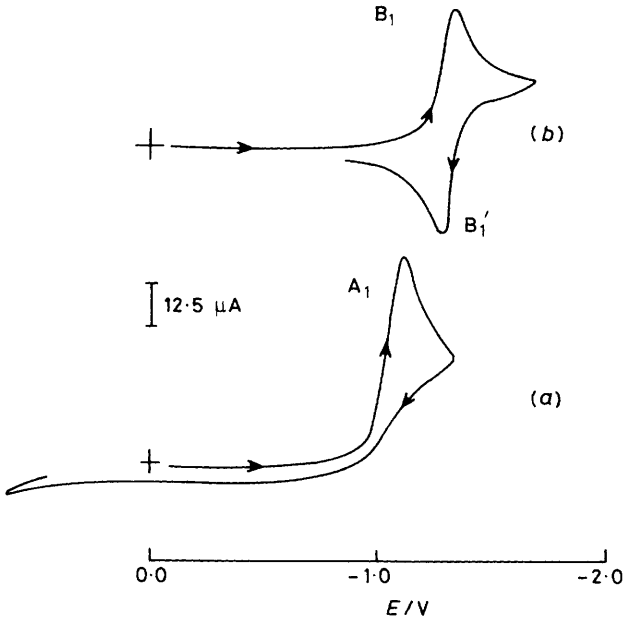

Figure 5. Cyclic voltammograms for (*a*) $[Cr(salen)(ox)]^-$ and (*b*) $[Cr(salen)(H_2O)_2]^+$. Details as in Figure 4

$[Fe^{III}(salen)(NO_3)]$ under the same experimental conditions [Figure 4(*b*)]. Accordingly, we assume that the cause of the irreversibility observed in the electrochemical behaviour of (**2**) is the existence of a rapid dissociation of the co-ordinated oxalate. Controlled-potential electrolysis and coulometry have been carried out. An oxidation wave (cyclic and rotating disc platinum electrode) at E_p = −0.32 V is clearly detected upon electrochemical reduction of (**2**) ($E_{applied}$ = 1.1 V), after the passage of 0.95 F per mol of complex. We assign this wave to the oxidation to the species Fe^{III}(salen). The relative intensity of the A_1 and A_2 peaks is affected by the presence of free oxalate in solution. If an excess of $[Hpip]_2[ox]$ is added to a solution of (**2**), the voltammogram changes immediately and the relative intensity of peak A_1 *versus* A_2 decreases. This feature is in accord with the existence of an equilibrium (8), the peaks A_1 and

$$2[Fe^{III}(salen)(ox)]^- \rightleftharpoons [Fe^{III}_2(salen)_2(ox)] + ox^{2-} \quad (8)$$

A_2 being due to the reduction of complexes (**2**) and (**3**) to Fe^{II}(salen). Although complexes (**2**) and (**3**) have similar metal-ion surroundings, the fact that the binuclear compound is more easily reduced than the mononuclear one is due to their different charges, which explains also that the cationic complex Fe^{III}(salen) is reduced at lower potential than (**2**) and (**3**).

Taking into account the above mentioned results we propose the reactivity pattern in Scheme 1.

Cyclic voltammetry on complex (**1**) in dmso shows an irreversible reduction peak A_1 at −1.10 V and, in contrast with the electrochemical behaviour observed for (**2**), no significant oxidation peaks are detected in the reverse sweep [Figure 5(*a*)]. Under the same conditions, the complex $[Cr^{III}(salen)(H_2O)_2]^+$ exhibits the typical voltammogram for a reversible system, E_p^{red} = −1.34 V ($\Delta E_p = E_p^c - E_p^a$ *ca.* 65 mV), Figure 5(*b*). The fact that $[Cr^{III}(salen)(ox)]^-$ is more easily reduced than $[Cr^{III}(salen)(H_2O)_2]^+$ indicates that the oxalate ligand stabilizes the chromium(II) complex in contrast with the behaviour of the Fe^{III}(salen)–oxalate system where the opposite situation was found. The lack of oxidation peaks in the reverse sweep for (**1**) can be interpreted on the basis of an inner-sphere redox of the complex $[Cr^{II}(salen)(ox)]^{2-}$ which would lead to Cr^{III}(salen) (stable at the potential of the peak A_1) and oxalate

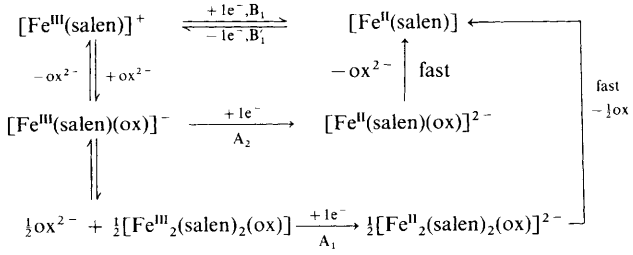

Scheme 1.

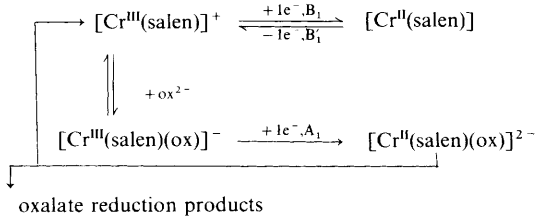

Scheme 2.

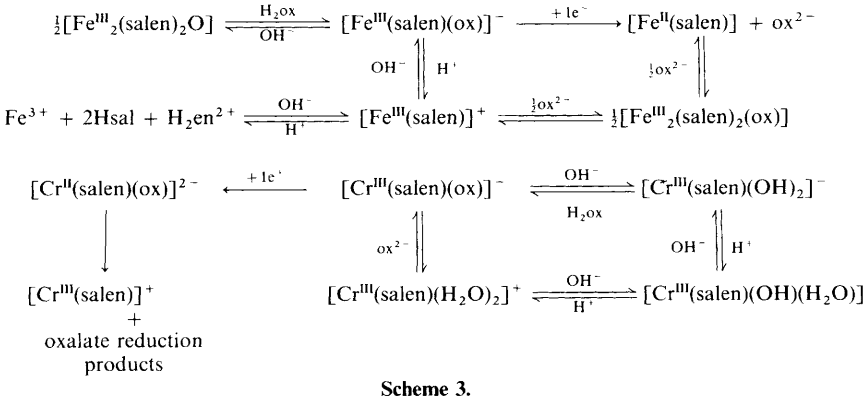

Scheme 3.

reduction products. This assumption is strongly supported by the detection of the species $[Cr^{III}(salen)(H_2O)_2]^+$ when cyclic voltammetry was carried out on solutions of $[Cr^{II}(salen)(H_2O)_2]$* to which oxalate has been added. Indeed, it has been shown that free oxalate is rather rapidly reduced to glycolate by solutions of chromium(II) perchlorate.[31] All these results allow us to propose the reactivity pattern in Scheme 2.

Electrochemical studies on chromium(III) complexes have shown that a linear relationship exists between the half-wave potential of the Cr^{III}–Cr^{II} couple and the 10*Dq* values. As the field strength of the ligands increases, a more negative potential is required for reduction.[32] Consequently, the fact that complex (**1**) is reduced more easily than $[Cr^{III}(salen)(H_2O)_2]^+$ could be attributed to the greater 10*Dq* value for the last compound.

The different chemical behaviour of the isostructural complexes (**1**) and (**2**) is illustrated by Scheme 3 which summarizes the chemical reactivity of these related systems.

Acknowledgements

We thank the Comisión Interministerial de Ciencia y Tecnología (Spain) for financial support of this work (PB85-0190).

* $[Cr^{II}(salen)(H_2O)_2]$ was generated by electrochemical reduction of $[Cr^{III}(salen)(H_2O)_2]^+$ at the potential of the peak B_1.

References

1 R. H. Heistand, II, R. B. Lauffer, E. Fikring, and L. Que, jun., *J. Am. Chem. Soc.*, 1982, **104**, 2789; R. B. Lauffer, R. H. Heistand, II, and L. Que jun., *ibid.*, 1981, **103**, 3947.
2 L. Que, jun., *Struct. Bonding (Berlin)*, 1982, **40**, 39.
3 R. B. Lauffer, R. H. Heistand, II, and L. Que, jun., *Inorg. Chem.*, 1983, **22**, 50.
4 (*a*) M. Calligaris, G. Nardin, and L. Randaccio, *Chem. Commun.*, 1969, 1248; (*b*) M. Calligaris, G. Manzini, G. Nardin, and L. Randaccio, *J. Chem. Soc., Dalton Trans.*, 1972, 543.
5 N. A. Bailey, B. M. Higson, and E. M. Mckenzie, *J. Chem. Soc., Dalton Trans.*, 1972, 503.
6 F. Lloret, J. Moratal, and J. Faus, *J. Chem. Soc., Dalton Trans.*, 1983, (*a*) 1743; (*b*) 1749.
7 F. Lloret, M. Mollar, J. Moratal, and J. Faus, *Inorg. Chim. Acta*, 1986, **124**, 67.
8 S. Yamada and K. Iwasaki, *Bull. Chem. Soc., Jpn.*, 1969, **42**, 1463.
9 D. Rajendra Prasad, T. Ramasami, D. Ramaswamy, and M. Santappa, *Inorg. Chem.*, 1980, **19**, 3181.
10 D. Rajendra Prasad, T. Ramasami, D. Ramaswamy, and M. Santappa, *Inorg. Chem.*, 1982, **21**, 850.
11 M. Julve and O. Kahn, *Inorg. Chim. Acta*, 1983, **76**, L39.
12 J. C. Fanning, J. L. Resce, G. C. Lickfield, and M. E. Kotun, *Inorg. Chem.*, 1985, **24**, 2884.
13 S. Yamada and K. Iwasaki, *Inorg. Chim. Acta*, 1971, **5**, 3.
14 P. Coggon, A. T. McPhail, F. E. Mabbs, A. Richards, and A. S. Thornley, *J. Chem. Soc. A*, 1970, 3296.
15 J. C. Bernier and P. Poix, *L'Actualité Chimique*, 1978, **2**, 7.

16 M. Mollar, Ph.D. Thesis, University of València, 1988.
17 P. Gans, A. Sabatini, and A. Vacca, *J. Chem. Soc., Dalton Trans.*, 1985, 1195.
18 P. Main, S. E. Fiske, S. L. Hull, L. Lessinger, G. Germain, J. Leclercq, and M. M. Woolfson, MULTAN 84, a System of Computer Programs for Crystal Structure Determination from *X*-Ray Diffraction Data, Universities of York, England and Louvain, Belgium, 1984.
19 G. M. Sheldrick, SHELX 76 Program for Crystal Structure Determination, Cambridge University, 1976.
20 'International Tables for *X*-Ray Crystallography,' Kynoch Press, Birmingham, 1974, vol. 4, pp. 99, 100, and 149.
21 A. M. Sargeson and G. H. Searle, *Inorg. Chem.*, 1965, **4**, 45.
22 R. H. Heistand, II, L. A. Roe, and L. Que, jun., *Inorg. Chem.*, 1982, **21**, 676.
23 M. Gerloch and F. E. Mabbs, *J. Chem. Soc. A*, 1967, 1900.
24 P. Herpin, *Bull. Soc. Fr. Mineral Cristallogr.*, 1958, **81**, 245.
25 J. N. van Niekerk and F. R. L. Schoening, *Acta Crystallogr.*, 1952, **5**, 196; R. H. Fenn, A. J. Graham, and R. D. Guillard, *Nature* (*London*), 1967, **213**, 1012; D. Taylor, *Aust. J. Chem.*, 1978, **31**, 1455.
26 J. Fujita, A. E. Martell, and K. Nakamoto, *J. Chem. Phys.*, 1962, **36**, 324.
27 C. K. Jørgensen, 'Absorption Spectra and Chemical Bonding in Complexes,' Pergamon, New York, 1962.
28 I. Morgenstern-Badarau, F. Lloret, and M. Julve, unpublished work.
29 H. Ogino, M. Shimura, and N. Tanaka, *Inorg. Chem.*, 1978, **18**, 2497 and refs. therein.
30 E. B. Fleisher and M. Krishnamurthy, *J. Am. Chem. Soc.*, 1971, **93**, 3784.
31 R. M. Milburn and H. Taube, *J. Phys. Chem.*, 1960, **64**, 1776.
32 A. A. Vlček, *Prog. Inorg. Chem.*, 1963, **5**, 353.

Received 21*st March* 1988; *Paper* 8/01147H